

## Neutralino Dark Matter Elastic Scattering in a Flat and Accelerating Universe

A. B. Lahanas<sup>1</sup>, D. V. Nanopoulos<sup>2</sup> and V. C. Spanos<sup>1</sup>

<sup>1</sup> *University of Athens, Physics Department, Nuclear and Particle Physics Section,  
GR-15771 Athens, Greece*

<sup>2</sup> *Department of Physics, Texas A & M University, College Station, TX 77843-4242,  
USA, Astroparticle Physics Group, Houston Advanced Research Center (HARC),  
Mitchell Campus, Woodlands, TX 77381, USA, and  
Academy of Athens, Chair of Theoretical Physics, Division of Natural Sciences,  
28 Panepistimiou Avenue, Athens 10679, Greece*

### Abstract

In SUGRA inspired supersymmetric models with universal boundary conditions for the soft masses, the scalar cross section  $\sigma_{scalar}$  for the elastic neutralino–nucleon scattering is in general several orders of magnitude below the sensitivity of current experiments. For large  $\tan\beta$  and low  $M_{1/2}, m_0$  values, the theoretically predicted  $\sigma_{scalar}$  can approach the sensitivity of these experiments ( $\approx 10^{-6} pb$ ) being at the same time in agreement with recent cosmological data, which impose severe restrictions on the CDM relic density, and with accelerator experiments which put lower bounds on sparticle and Higgs boson masses. Further improvement of the sensitivity of DAMA and CDMS experiments will probe the large  $\tan\beta$  region of the parameter space in the vicinity of the boundaries of the parameter space allowed by chargino and Higgs searches.

As time goes by there is indisputable, accumulative experimental (observational) evidence that we live in a flat and accelerating universe. Indeed, the most recent confirmation of such a dramatic statement have been the new results from the BOOMERANG [1] and MAXIMA [2] experiments, where for the first time, it has been possible to measure several crucial cosmological parameters simultaneously. The position of the first acoustic peak of the angular power spectrum strongly suggests that  $\Omega_0 = 1$  (i.e.  $k = 0$ , a flat universe), while its shape is consistent with the predicted inflationary density perturbations. It is rather heartwarming to see the way that the data favour an almost flat Universe  $\Omega_0 \equiv \Omega_M + \Omega_\Lambda = 1 \pm 0.2$  [3] where  $\Omega_M$  is contribution of the matter density and  $\Omega_\Lambda$  is that of the vacuum energy. At the same time one determines that  $\Omega_M = 0.4 \pm 0.1$  which in conjunction with analysis from high- $z$  SNa data result to  $\Omega_\Lambda = \frac{4}{3} \Omega_M + \frac{1}{3} \pm \frac{1}{6}$  [4]. With  $\Omega_M = 0.4 \pm 0.1$  this implies that  $\Omega_\Lambda = 0.85 \pm 0.2$  [3]. Taking into account the fact that the baryonic contribution to the matter density is small,  $\Omega_B = 0.05 \pm 0.005$ , the values for matter energy density  $\Omega_M$  result to a Cold Dark Matter (CDM) density  $\Omega_{\text{CDM}} \simeq 0.35 \pm 0.1$ , which combined with more recent measurements of the scaled Hubble parameter  $h_0 = 0.65 \pm 0.05$ , result to small CDM relic densities  $\Omega_{\text{CDM}} h_0^2 \simeq 0.15 \pm 0.07$  [3]. Combined analysis from MAXIMA, BOOMERANG and COBE/DMR data entails to even tighter limits [5], though we are not using such stringent limits trying not to extremely constrain the parameter space of the MSSM.

While the cosmological picture seems to be brighten up at least at the level of a phenomenological understanding, we are facing some squeezing at the other end, i.e. at the fundamental particle physics front. The question of “who ordered this?” for the cosmological constant is so obvious that needs no further elaboration. On the other hand the “observed” value of  $\Omega_M$  cries out for an non-baryonic component, rather difficult to be provided by the nearly massless neutrinos, if we take at face value the present values of neutrino masses.

In  $R$ -parity conserving supersymmetric theories the lightest supersymmetric particle (LSP or  $\tilde{\chi}$ ) may be a neutralino, which is a good candidate to play the role of dark matter (DM) particle. While it is very encouraging that the neutralino parameters (masses, couplings) are in the right range to provide easily the right amount of DM, e.g. the “correct” contribution to  $\Omega_M$ , neutralinos still have escaped any direct or indirect detection so far. The direct way to detect the neutralino is via the neutralino–nucleus scattering. This scattering contains spin-dependent as well as spin-independent (scalar) parts. For the heavy nuclei detectors the spin-independent part dominates, because there neutron and proton scattering amplitudes are approximately equal. The present sensitivity of experi-

ments DAMA [6] and CDMS [7] measuring the spin-independent neutralino–proton cross section  $\sigma_{scalar}$ , is approximately  $10^{-5} - 10^{-6} pb$ . The CDMS collaboration has reported negative results from their experiments [7], setting an upper limit on the spin-independent  $\sigma_{scalar}$  that excludes also almost all the range suggested by the DAMA collaboration [6]. Thus in this letter we focus our interest mainly in the CDMS limits.

Since neutralinos seem to play a very important *link* between the very-very small (SUSY theories) and the very-very large (DM) it is imperative at every stage to have an *integrated* picture of what is allowed and what it isn't. During the last year we have embarked in such an effort [8], having used cosmological data and electroweak (EW) precision data (mainly from LEP) to constrain, in generic SUSY theories, the parameter space. In this letter we continue our programme [8] by injecting the new cosmological data and new SUSY bounds into our analysis but take also into account the most recent CDMS direct-search exclusion limits.

As we shall see, in general, one has to improve considerably the sensitivity of the direct-search limits in order to start excluding sections of the otherwise allowed parameter space. DM detectors have a current sensitivity  $\approx 10^{-5} - 10^{-6} pb$  and would be interesting to find regions of the MSSM parameter space where bounds imposed by CDMS experiments are nearly saturated. In most of the parameter space the scalar LSP nucleon cross section  $\sigma_{scalar}$  is small getting values as small as  $\approx 10^{-9} pb$  or even less for LSP masses  $m_{\tilde{\chi}} \approx 200$  GeV. This indicates that DAMA and CDMS data at the current stage are not that useful to probing MSSM with universal boundary conditions (UBC) for the soft masses at the Unification scale. Relaxing the UBC can result to enhancement of the  $\sigma_{scalar}$  as has been studied in Refs [9–11].

Our purpose in this paper is to keep on UBC for all soft masses and focus mainly on points that are compatible with neutralino relic densities within the cosmologically allowed domain  $\Omega_{\tilde{\chi}} h_0^2 = 0.15 \pm 0.07$ , which yield cross sections  $\sigma_{scalar}$  close to the boundary of the area excluded by CDMS experiments. For low  $\tan\beta < 20$  this is unlikely to occur but for higher values cross sections increase with  $\tan\beta$  due to the fact that Higgs bosons become lighter [10]. It is interesting to point out that large  $\tan\beta$  offers an alternative to neutralino–stau coannihilation mechanism to decrease neutralino relic densities, in cases the LSP is a high purity bino. Its small Higgsino component is very important since it allows it to couple with the pseudoscalar Higgs boson  $A$  with a strength that becomes sizable for large  $\tan\beta$  despite the smallness of the LSP's Higgsino composition. This in combination with the fact that  $A$  mass decreases with large  $\tan\beta$ , making pseudoscalar exchanges less suppressive, can lead to sizable  $\tilde{\chi} \tilde{\chi} \rightarrow b \bar{b}$  and  $\tilde{\chi} \tilde{\chi} \rightarrow \tau \bar{\tau}$  cross sections

and hence low relic densities. This has been emphasized in Ref. [8]. Although the role of the pseudoscalar  $A$  is very significant for this mechanism,  $A$  itself plays no important role in  $\sigma_{scalar}$  except that its mass is simultaneously decreased, as  $\tan\beta$  grows, with that of the heaviest of the  $CP$ -even Higgses which does mediate the neutralino–nucleon elastic cross section. Therefore it would be interesting to perform a refined scan of the parameter space, for large  $\tan\beta$ , to search for points which lead to both small relic densities and values of  $\sigma_{scalar}$  in the vicinity of the boundary excluded by CDMS data.

In our analysis we assume UBC for the soft masses and focus mainly to large  $\tan\beta$  although results for low  $\tan\beta$  will be also reported. In our evaluation of the scalar cross section  $\sigma_{scalar}$  we are using the formulae of Ref. [12]. For the hadronic matrix elements we use the values of the Ref. [11].

Regarding the mass of the pseudoscalar boson which plays an important role in decreasing the LSP relic density a subtlety arises related to the theoretical determination of its mass which we should now discuss. It is well known that radiative corrections to its mass usually calculated through the effective potential approach are not stable with changing the scale at which they are calculated. Empirically one calculates its mass at an average scale  $Q_t$  for which the radiative corrections to its mass, due to the third generation sfermions, are small and hence can be neglected. In this scheme the pseudoscalar mass squared is given by  $m_A^2 = -2 m_3^2(Q_t)/\sin 2\beta(Q_t)$ , where  $m_3^2$  is the Higgs mixing parameter. Although this is in principle correct contributions of charginos and neutralinos are not small at this scale especially when  $M_{1/2}$  is large. In some case this may produce an error in the determination of its mass as large as 25%. Excluding the chargino/neutralino contribution is legitimate provided the relevant scale is not taken to be  $Q_t$ , but rather the average chargino/neutralino mass  $Q_{inos}$ . At this scale their contributions can be safely neglected. This scale however may differ substantially from  $Q_t$ , when  $M_{1/2}$  is large, and third generation contributions are not small if they are calculated at  $Q_{inos}$ . In our approach for the determination of the pseudoscalar’s mass we have duly taken into account all contributions including the chargino/neutralino corrections, as well as the small gauge and Higgs boson contributions, and have observed that they contribute significantly to the stabilization of the pseudoscalar Higgs boson mass with changing the scale  $Q$ . If these contributions were neglected stabilization would be spoiled especially in the large  $M_{1/2}$  region where the running of the parameter  $m_3^2(Q)$  due to gauginos becomes important and their corrections should be included to render a  $Q$  independent result. The situation would be even more dramatic if in addition to having large  $M_{1/2}$  we are in the large  $\tan\beta$  regime where such deviations from stability are enhanced as being proportional to  $\tan\beta$ .

It is also well known that the mass calculated through the effective potential differs from the pole mass by  $\Pi(0) - \Pi(m_A^2)$ , where  $\Pi(p^2)$  denotes the corrections to the pseudoscalar propagator. For a more reliable estimation of the pseudoscalar's mass we have also included the leading logarithmic parts of  $\Pi(0) - \Pi(m_A^2)$  to the effective potential mass leaving aside unimportant, at least for our analysis, small corrections. In this way we have approximated satisfactorily the pole mass and avoid the complexities of calculating one-loop integrals, which are usually expressed by Passarino–Veltman functions, as would be demanded if we were to determine the pseudoscalar mass through the location of the pole of the propagator [13].

For consistency, both for the calculation of the pseudoscalar mass and for determining the Higgsino and Higgs mixing parameters  $\mu, m_3^2$  through the one-loop minimization conditions, we take into account the contribution of all sectors to the derivatives of the effective potential not just those of the third generation. These are given in Ref. [14]. Since however they are given in the Landau gauge, while we are using two-loop RGE's in the 't Hooft's gauge, we remedy this situation by using the gauge and Higgs boson contributions to the minimization conditions as these follow directly from the tadpole graphs calculated in the 't Hooft's gauge, as can be found in Ref. [15]. More details can be found in Ref. [13].

Regarding the neutralino relic density we calculate it in the way prescribed in Ref. [8]. We solve numerically the Boltzmann transport equation ignoring at the first stage coannihilation effects [16], and in particular  $\tilde{\tau} - \tilde{\chi}$  and in general  $\tilde{l} - \tilde{\chi}$  coannihilation effects [17]. The latter are important for a bino like LSP when its mass is close to that of the lightest of the  $\tilde{\tau}$ . The importance of these in reducing the relic density has been stressed in Refs [17]. One can include the contribution of the coannihilation processes, whenever they are of relevance, following the empirical rule

$$\Omega_{\tilde{\chi}} = R(\Delta M) \Omega_{\tilde{\chi}}^0. \quad (1)$$

The reduction factor  $R(\Delta M)$  depends on  $\Delta M = (m_{\tilde{\tau}_R} - m_{\tilde{\chi}})/m_{\tilde{\chi}}$  and the function  $R(\Delta M)$  smoothly interpolates between  $\approx 0.1$  and 1.0 for values of  $\Delta M$  in the range 0.00 – 0.25 (see Ref. [8]). The equation above is a handy device and reproduces the results cited in Ref. [17].  $\Omega_{\tilde{\chi}}^0$  appearing on the r.h.s. of the equation above is the relic density calculated ignoring coannihilation channels. All effects of coannihilation processes are effectively included within the function  $R$ .

As a preview of our results, we have found that the largest  $\sigma_{scalar}$ , approaching values  $10^{-6} - 10^{-7} pb$ , are obtained in regions of parameter space for which  $\tan\beta$  is large. The dominant contribution to this regime is the Higgs boson exchange. For given inputs

$m_0, M_{1/2}, A_0$  and the sign of  $\mu$ , Higgs masses decrease as  $\tan\beta$  increases. The maximum value of this angle is determined by the theoretical requirement that we are at the correct electroweak minimum and Higgs masses squared are positive and bounded from below by the recent experimental limits [18]. Hence the contribution of Higgs bosons to neutralino–quark elastic cross section becomes more important in the large  $\tan\beta$  regime. Such a decrease in the mass is not sufficient by itself to increase  $\sigma_{scalar}$  to levels approaching the sensitivity of ongoing experiments. The major role in this increase plays the coupling of the  $CP$ -even heavy Higgs whose coupling to  $d$ -quark is proportional to  $\frac{\cos\alpha}{\cos\beta}$ . This is proportional to  $\tan\beta$ , when the latter becomes large, since  $\cos\beta \approx 1/\tan\beta$  and the Higgs mixing angle  $\alpha$  becomes small and negative in this region resulting to  $\cos\alpha \approx 1$ . The situation alters for the light  $CP$ -even Higgs boson whose coupling is  $\frac{\sin\alpha}{\cos\beta}$ . In this case  $\sin\alpha$  behaves as  $1/\tan\beta$  and unlike the heavy Higgs case its coupling does not grow with increasing  $\tan\beta$  but stays constant of order unity. Therefore despite the fact that the heavy  $CP$ -even Higgs is heavier than its light  $CP$ -even counterpart, its contribution may be much larger in the large  $\tan\beta$  region, due to its enhanced coupling to  $d$ -quark [19].

From the above argument we conclude that points of the parameter space that are likely to yield the highest possible elastic cross sections are those for which  $\tan\beta$  is large and the heavy  $CP$ -even state receives its minimum value allowed by experiments and other theoretical constraints. The contributions of sfermion exchanges to the amplitude of the elastic cross sections are less important and will not be discussed. In the constrained supersymmetric scenario the mass of the  $CP$ -even heavy state  $m_H$ , has the tendency to increase with increasing the effective supersymmetry scale and therefore low  $m_H$  values are obtained for low  $m_0, M_{1/2}$  values. The mass  $m_H$  is bounded by the mass of the light Higgs boson  $m_h$  since

$$m_H^2 = m_h^2 + \left[ \frac{1}{4} ((m_A^2 + m_Z^2)^2 + \epsilon^2) - m_A^2 m_Z^2 (\cos 2\beta)^2 + \frac{\epsilon}{2} \cos 2\beta (m_A^2 - m_Z^2) \right]^{1/2}. \quad (2)$$

In this expression  $m_A$  refers to the radiatively corrected pseudoscalar Higgs boson mass and  $\epsilon$  are the leading stop corrections to the  $CP$ -even Higgs masses. Allowing for additional non-leading contributions, or for contributions from other sectors, the expression above is modified but for the sake of clarity in presenting our arguments we will use the simplified relation as presented above. In our numerical analysis we have duly taken into account all stop corrections to the  $CP$ -even mass matrix as well as those of sbottoms and staus.

In the large  $\tan\beta$  regime  $\cos 2\beta \approx -1$  and the relation above is simplified to

$$m_H^2 = m_h^2 + \frac{1}{4}(m_A^2 - m_Z^2 - \epsilon). \quad (3)$$

Obviously the lowest  $m_H$  values are obtained in the region where  $m_A$  is light and  $m_h$  is close to its lower experimental bound. The value of  $\epsilon$  can also decrease the mass  $m_H$ , however this depends logarithmically on the stop masses and unlike  $m_A$  does not vary much with changing the SUSY breaking parameters  $m_0, M_{1/2}$  and can be considered practically stable. Since Higgs masses increase with increasing the parameters  $M_{1/2}, m_0$  and get lowered with increasing  $\tan\beta$ , the region of interest the most likely to yield scalar cross sections nearly saturating the sensitivity of current CDMS experiments is the region of large  $\tan\beta$  and low  $M_{1/2}, m_0$  close to the boundaries allowed by Higgs boson and chargino searches. It becomes evident that increase of the sensitivity of CDMS experiments will probe this region and may exclude points that would be otherwise allowed by accelerator experiments.

It is worth pointing out that in the large  $\tan\beta$  region neutralino relic densities decrease as we have already emphasized due to both the decrease of the pseudoscalar mass, whose exchange in  $\tilde{\chi}\tilde{\chi} \rightarrow b\bar{b}$ ,  $\tau\bar{\tau}$  processes is less suppressive, and the increase of the  $\tilde{\chi}\tilde{\chi}A$  coupling. The smallness of the LSP's Higgsino component is compensated by the largeness of  $\tan\beta$  yielding neutralino annihilation cross sections compatible with the recent astrophysical data when  $M_{1/2}$  gets values  $< 200$  GeV [8]. Hence there are regions in which we can obtain both low relic densities and high  $\sigma_{scalar}$  and these regions can be possibly probed by the next round CDMS experiments.

For our numerical analysis we have scanned regions of parameter space with values  $\tan\beta = 1.8 - 50$ ,  $M_{1/2} < 1350$  GeV,  $m_0 < 1$  TeV,  $|A_0| < 500$  GeV. The dependence on  $A_0$  is rather mild and for this reason we cut points with values  $|A_0| > 500$  GeV. In Figure 1 we display the behavior of  $\sigma_{scalar}$  for both positive and negative values of the parameter  $\mu$  for given  $m_0 = 200$  GeV,  $A_0 = 0$  GeV and values of  $M_{1/2} = 200, 400$  and  $600$  GeV respectively. One observes that for  $M_{1/2} = 200$  GeV, which is close to the minimum value allowed by chargino searches ( $M_{1/2}|_{min} \approx 170$  GeV), the scalar cross section increases with increasing  $\tan\beta$ . Especially in the  $\mu < 0$  case this increase is more steep and  $\sigma_{scalar}$  can reach values slightly above  $10^{-6}$  pb. In the other cases shown, corresponding to  $M_{1/2} = 400, 600$  GeV, the situation is quite different and  $\sigma_{scalar}$  gets smaller by at least an order of magnitude, due to the heaviness of all sectors involved, with the exception of the light Higgs whose contribution in this region is however small. The abrupt stop of all lines towards their right endings occurs since for higher values of  $\tan\beta$  we enter regions which are theoretically excluded. Towards the left endings of these lines the light Higgs mass approaches its lowest experimental bound  $\approx 110$  GeV. For the negative  $\mu$  case a steep deep is observed for  $M_{1/2} = 400, 600$  GeV and  $\tan\beta = 10$ .

This is accidental and due to the cancellation of sfermion and Higgs contributions to the amplitudes of the elastic  $\tilde{\chi}$ -nucleon cross section [11].

In Figure 2 we plot the scalar cross section as function of the LSP mass  $m_{\tilde{\chi}}$ . Each point, struck by either a plus or a cross, has been picked from a sample of 5000 random points in the region of parameter space mentioned previously. We simultaneously calculate the neutralino relic density and we denote points which are cosmologically allowed,  $\Omega_{\tilde{\chi}} h_0^2 = 0.15 \pm 0.07$ , by a plus and those which are not allowed by a cross symbol. In this random sample the relic density is calculated without taking into account the coannihilation processes. We shall return to this point later. From this figure it is seen that irrespectively of the value of the relic density, points that have large cross sections  $\approx 10^{-6} pb$  correspond to LSP masses  $m_{\tilde{\chi}} < 80$  GeV, or equivalently values of  $M_{1/2}$  less than about 200 GeV, that is in the region near the edge allowed by recent chargino searches. Moreover these points are characterized by large  $\tan\beta$  ( $> 30$ ). Some remarks are in order. The first concerns the blank stripe occurring at values of  $m_{\tilde{\chi}}$  near 175 GeV. This indicates the presence of a top threshold in  $\tilde{\chi}\tilde{\chi} \rightarrow t\bar{t}$  annihilation cross section. This appears because in order to speed up calculations we have avoided calculating the relic density at singular points, near thresholds or poles, where non-relativistic expressions usually employed break down, and more refined techniques must be used to get the correct result. Besides this we observe the development of other stripes too in the vicinity of  $\approx 100$  GeV which correspond to poles of Higgses and other sparticles involved.

The void region in the negative  $\mu$  case for values  $100 \lesssim m_{\tilde{\chi}} \lesssim 280$  GeV, is due to the fact that for given value of  $\tan\beta$ ,  $m_0$  and  $A_0$ , an upper bound is set on  $M_{1/2}$ , or equivalently  $m_{\tilde{\chi}}$ , beyond which we run into situations where EW symmetry is not broken to the correct vacuum. The larger the value of  $\tan\beta$  is the lower the value of the upper bound of  $M_{1/2}$  is. Hence points of the sample that yield large cross section for low  $M_{1/2}$  values, for values higher than the upper bound set on  $M_{1/2}$  are completely absent from the figure since are automatically excluded. The dispersed points appear for large values of  $M_{1/2}$  in the  $\mu > 0$  case are related with the behavior of the  $\sigma_{scalar}$  as a function of  $\tan\beta$  for large values of  $M_{1/2}$ . Actually for such large values of  $M_{1/2}$  the light Higgs boson exchange dominates the  $\tilde{\chi}q \rightarrow \tilde{\chi}q$  process and therefore the  $\sigma_{scalar}$ . However this contribution is proportional to the  $\tilde{\chi}\tilde{\chi}h$  coupling, which varies very much with the  $\tan\beta$  for large values of  $M_{1/2}$ , resulting to the dispersion shown in the figure.

Figure 3 follows from Figure 2 if we discard points that do not fall within the cosmologically allowed region  $\Omega_{\tilde{\chi}} h_0^2 = 0.15 \pm 0.07$ . We observe that only a few points survive for both negative and positive  $\mu$  cases when we enforce this strict cosmological



bound on the relic density. Since we have so far neglected coannihilation processes in our analysis, and especially  $\tilde{\tau} - \tilde{\chi}$  which are the important ones when  $\tilde{\chi}$  is mostly a bino, this sample is expected to be enriched when these processes are taken into account. This is done in Figure 4 where it is shown that the sample of cosmologically allowed points is indeed enriched but not in the region which yields the largest possible cross sections. The relic density for points that coannihilation processes are of relevance are calculated as explained in the general discussion earlier in this paper.

In Figures 5 we display  $\sigma_{scalar}$  as function of  $\tan\beta$  for the random points disused in the previous figures. It is seen that points in the large  $\tan\beta$  region approach  $10^{-6} pb$ , in the case  $\mu > 0$ , and can slightly exceed this value for  $\mu < 0$ . These are characterized by large  $\tan\beta$  and low  $m_0, M_{1/2}$  values and are in agreement with accelerator experiments on sparticle and Higgs searches. Some of these points can survive the strict relic density bounds indicating that an improvement of the sensitivity of CDMS experiments can explore the parameter space of MSSM with large  $\tan\beta$  and low  $m_0, M_{1/2}$ . Large  $\tan\beta$  for  $\mu > 0$  are also compatible with  $b \rightarrow s + \gamma$  data from CLEO [20], and hence next run CDMS experiments may be capable of imposing bounds relevant to regions of parameter space which accelerator experiments have not probed as yet.

Concluding we have seen that in order to have as large  $\sigma_{scalar}$  as possible and close to CDMS experiment sensitivity, that is  $10^{-6} - 10^{-7}$ ,  $M_{1/2}$  must be as small as allowed by chargino searches and  $\tan\beta$  as large as possible for the Higgs states to be as light as allowed by theoretical constraints and experimental searches. This happens both for  $\mu > 0$  and  $\mu < 0$ . In addition in the  $\mu > 0$  case we can also obtain large  $\sigma_{scalar}$  for large  $M_{1/2} \sim 1$  TeV, again for large  $\tan\beta \gtrsim 30$ , but these points tend to give unacceptably large relic densities,  $\Omega_{\tilde{\chi}} h_0^2 > 1$ . On the other hand for  $\mu < 0$  and large  $\tan\beta$ , we can get large  $\sigma_{scalar}$  for moderate values of  $M_{1/2} \sim 450$  GeV, which are cosmologically acceptable. In all cases considered the necessary condition in order to have  $\sigma_{scalar} \sim 10^{-6} - 10^{-7}$  is that  $\tan\beta \gtrsim 35$ , as can be clearly seen from Figure 5. It is perhaps important to note that although the  $\mu < 0$  case yields, in general, larger cross sections than the  $\mu > 0$  case, the former is disfavoured in view of  $b \rightarrow s + \gamma$  experimental data [20].

## Acknowledgments

A.B.L. acknowledges support from ERBFMRXCT-960090 TMR programme and D.V.N. by D.O.E. grant DE-FG03-95-ER-40917. V.C.S. acknowledges support from Academy of Athens under 200/486-2000 grant and from European Union under contract HPRN-CT-2000-00149. The authors wish to express their thanks to the CDMS collaboration for communications.

**Note added :**

After submitting this paper for publication we became aware of the paper hep-ph/0012377 by Bottino, Fornego and Scopel in which values for the scalar neutralino-nucleon cross section ( $\sigma_{scalar}$ ) are obtained which can explain the DAMA data. The region of the parameter space in this paper in the case of the mSUGRA model is extended to values of  $m_0$  up to 3 TeV. In our paper we have taken values for the  $m_0$  parameter not exceeding 1 TeV. This range is the same with that explored in the paper hep-ph/0010203 by Bottino, Donato, Fornego and Scopel. The conclusions reached in that paper are in agreement with those presented in our work (see figure 1a of the aforementioned article). Increasing the upper limit of  $m_0$  to include values 1 TeV, we enter regions in which acceptable neutralino relic densities are obtained with higher values for  $\sigma_{scalar}$ , falling within the DAMA experimental sensitivity, at the cost of having a very massive sfermion spectrum. The region  $m_0 > 1$  TeV with  $M_{1/2} < 600$  GeV characterizes the “Focus Point Supersymmetry” ( see the references J. Feng, K. Matchev and F. Wilczek, Phys. Lett. B482 (2000) 388; J. Feng and K. Matchev, Phys. Rev. D63 (2001) 095003). Nevertheless it should not escape our attention the fact that the “focus point” region is now disallowed by the BNL E821 experiment (H. N. Brown *et al.*, *Muon  $g-2$  collaboration*, hep-ex/0102017 ) and other constraints as emphasized recently in Ref. hep-ph/0102331 on  $g - 2$  (J. Ellis, D. V. Nanopoulos and K. Olive, hep-ph/0102331).

## References

- [1] P. de Bernardis *et al.*, Nature 404 (2000) 995.
- [2] S. Hanany *et al.*, astro-ph/0005124.
- [3] M. Turner, astro-ph/9904051; astro-ph/9912211 and references therein.
- [4] S. Perlmutter *et al.*, Nature 391 (1998) 51; A. G. Riess *et al.*, Astron. J. 116 (1998) 1009; M. White, Astrophys. J. 506 (1998) 495.
- [5] A.H. Jaffe *et al.*, astro-ph/0007333; M. Tegmark, M. Zaldarriaga and A.J.S. Hamilton, astro-ph/0008167; hep-ph/0008145.
- [6] R. Bernabei *et al.*, DAMA Collaboration, Phys. Lett. B480 (2000) 23.
- [7] R. Abusaidi *et al.*, CDMS Collaboration, Phys. Rev. Lett. 84 (2000) 5699.
- [8] A.B. Lahanas, D.V. Nanopoulos and V.C. Spanos, Phys. Lett. B464 (1999) 213; Phys. Rev. D62 (2000) 023515.
- [9] A. Bottino, F. Donato, N. Fornengo and S. Scopel, Phys. Rev. D59 (1999) 095003; Phys. Rev. D59 (1999) 095004.
- [10] E. Accomando, R. Arnowitt, B. Dutta and Y. Santoso, hep-ph/0001019.
- [11] J. Ellis, A. Ferstl and K.A. Olive, Phys. Lett. B481 (2000) 304; hep-ph/0007113.
- [12] M. Drees and M.M. Nojiri, Phys. Rev. D48 (1993) 3483; G. Jungman, M. Kamionkowski and K. Griest, Phys. Rep. 267 (1996) 195.
- [13] A. Katsikatsou, A.B. Lahanas, D.V. Nanopoulos and V. C. Spanos, in preparation.
- [14] R. Arnowitt and P. Nath, Phys. Rev. D46 (1992) 3981.
- [15] V. Barger, M.S. Berger and P. Ohmann, Phys. Rev. D49 (1994) 4908; J. Bagger, K. Matchev, D. Pierce and R. Zhang, Nucl. Phys. B491 (1997) 3; J. Erler and D. Pierce, Nucl. Phys. B526 (1998) 53.
- [16] P. Binetruy, G. Giraldi and P. Salati, Nucl. Phys. B237 (1984) 285; K. Griest and D. Seckel, Phys. Rev. D43 (1991) 3191; P. Gondolo and G. Gelmini, Nucl. Phys. B360 (1991) 145; S. Mizuta and M. Yamaguchi, Phys. Lett. B298 (1993) 120; M. Drees, M.M. Nojiri, D.P. Roy and Y. Yamada, Phys. Rev. D56 (1997) 276; J. Edsjö and

- P. Gondolo, Phys. Rev. D56 (1997) 1879; P. Gondolo and J. Edsjö, hep-ph/9711461, Talk presented by P. Gondolo at “Topics in Astroparticle and Underground Physics (TAUP) ’97”, Laboratori Nazionali del Gran Sasso – Italy, 7-11 September 1997.
- [17] J. Ellis, T. Falk and K.A. Olive, Phys. Lett. B413 (1998) 355; J. Ellis, T. Falk, K.A. Olive and M. Srednicki, Astropart. Phys. 13 (2000) 181.
- [18] D.E. Groom *et al.* (Particle Data Group), Eur. Phys. Jour. C15 (2000) 1, URL: <http://pdg.lbl.gov>.
- [19] R. Arnowitt and P. Nath, Phys. Rev. D54 (1996) 2374.
- [20] H. Baer, M. Brhlik, D. Castaño and X. Tata, Phys. Rev. D58 (1998) 015007.

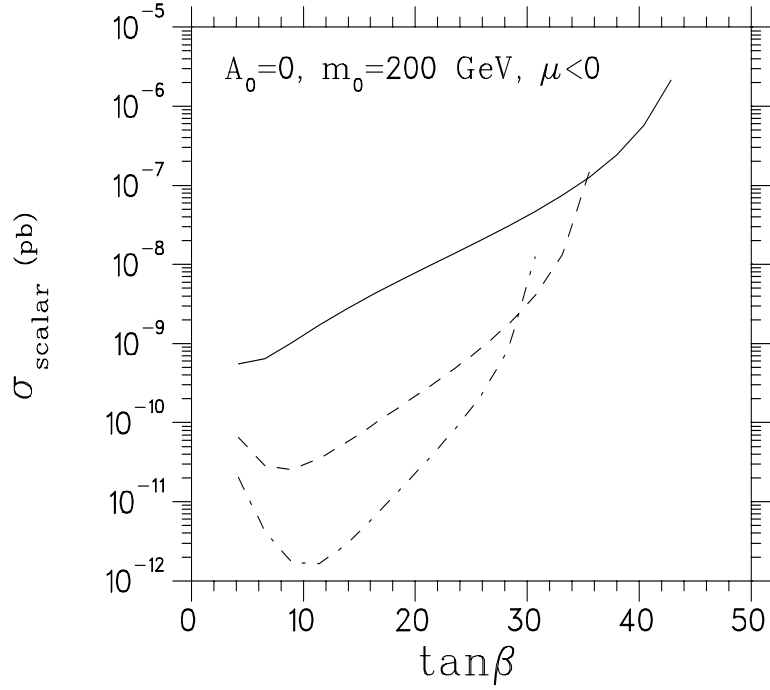
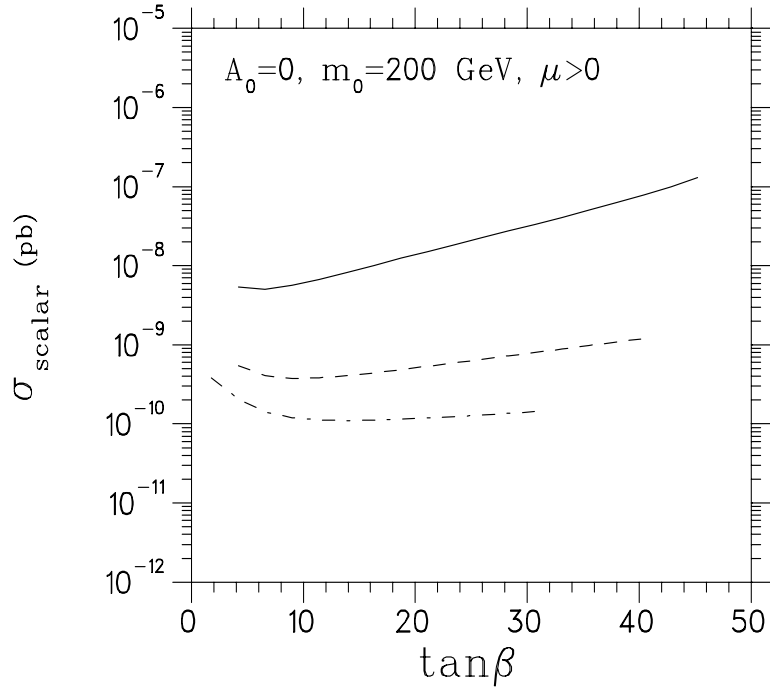


Figure 1: The  $\sigma_{\text{scalar}}$ , as function of  $\tan\beta$ , for both positive and negative values of the parameter  $\mu$  for given  $m_0 = 200 \text{ GeV}, A_0 = 0 \text{ GeV}$ . The solid, dashed and dot-dashed lines correspond to  $M_{1/2} = 200, 400$  and  $600 \text{ GeV}$  respectively.

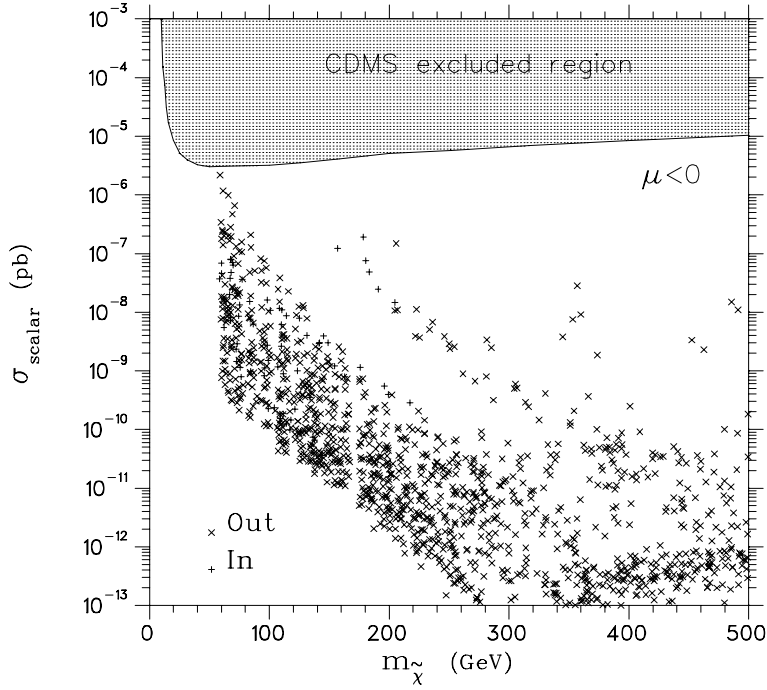
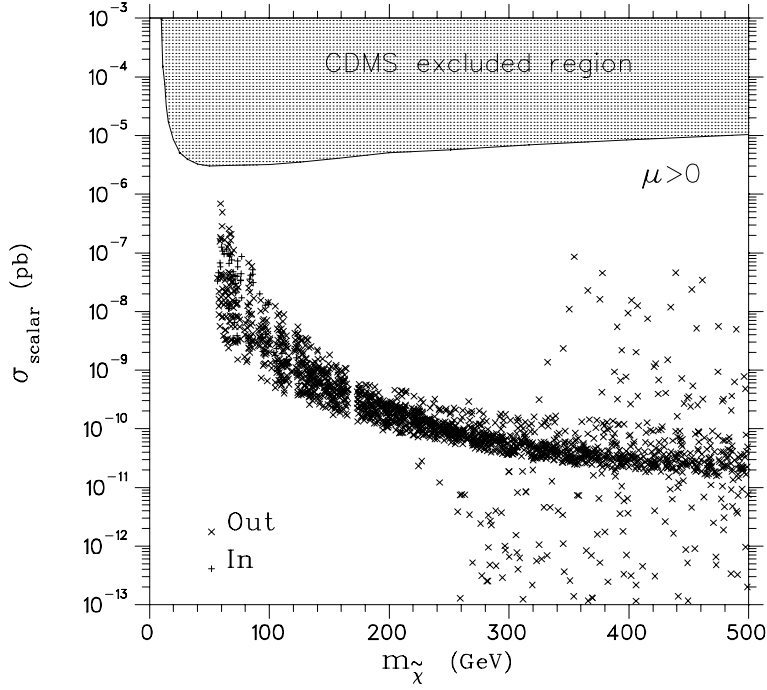


Figure 2: Scattered plot of the  $\sigma_{scalar}$  versus  $m_{\tilde{\chi}}$  from a sample of 5000 random points in the parameter space. Both cosmologically acceptable,  $\Omega_{\tilde{\chi}} h_0^2 = 0.15 \pm 0.07$  (marked as “In”), and unacceptable points (marked as “Out”) are plotted. Low  $m_{\tilde{\chi}}$  values are excluded by chargino searches. The shaded region on the top is excluded by CDMS experiment [7].

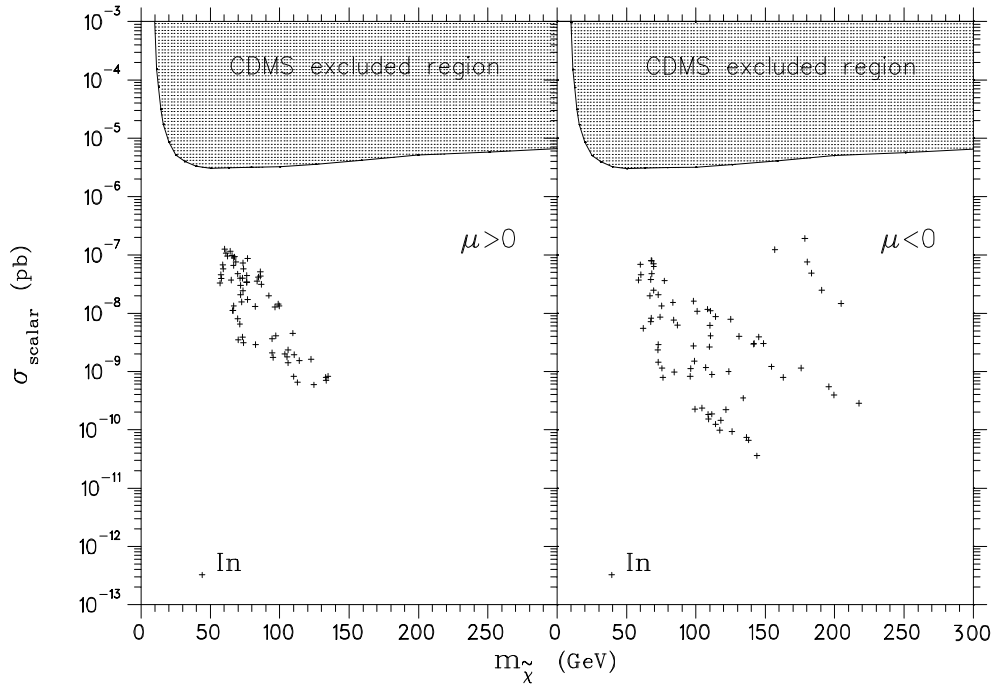


Figure 3: The same as in Figure 2, where only the cosmologically acceptable points are plotted.

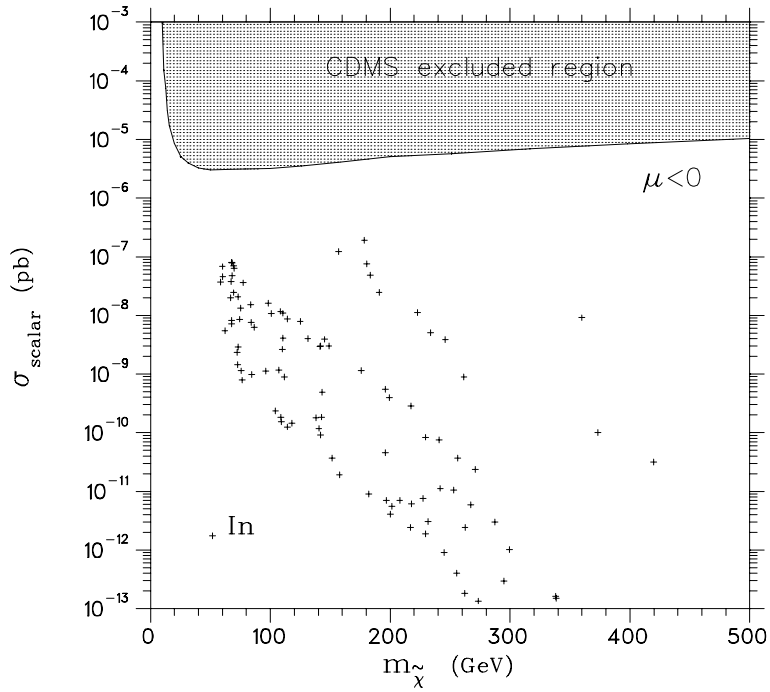
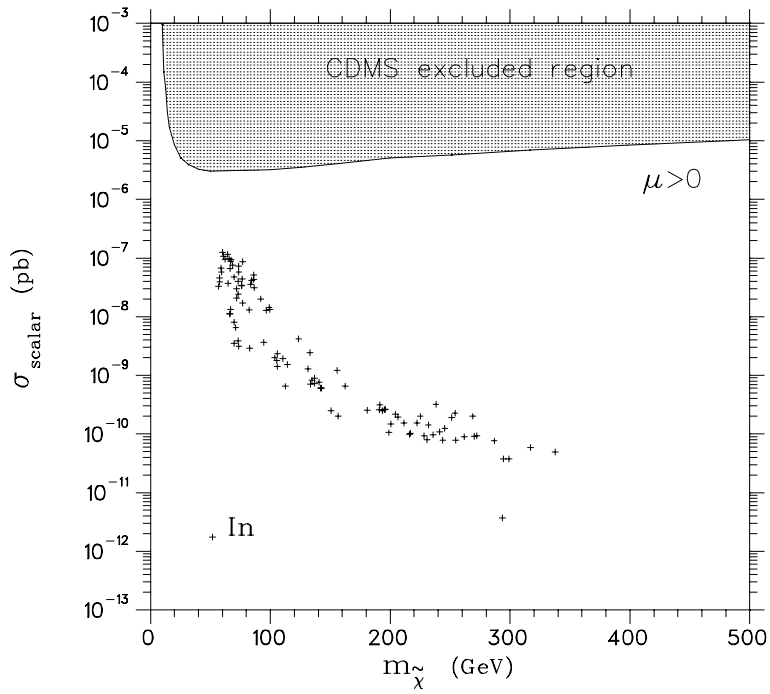


Figure 4: The same as in Figure 3, where the coannihilation corrections are taken into account.



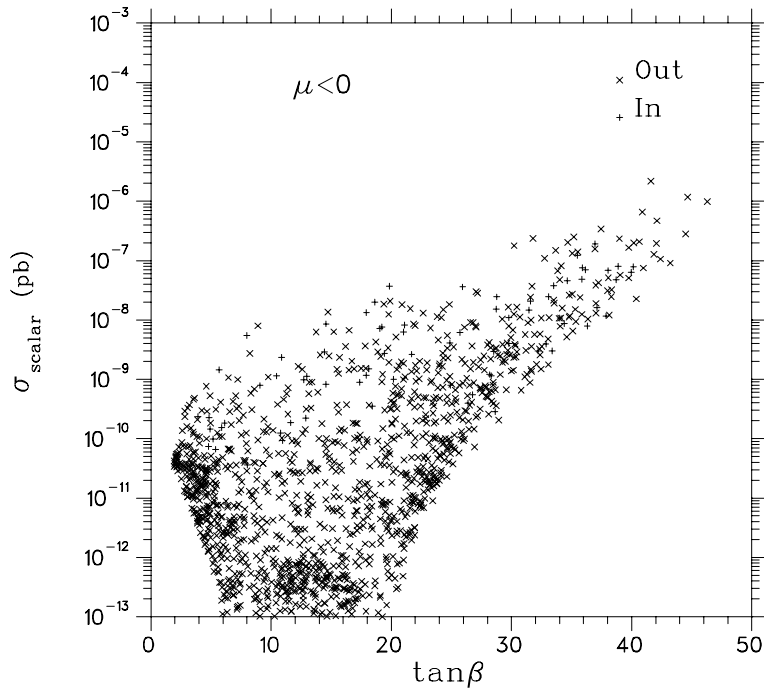
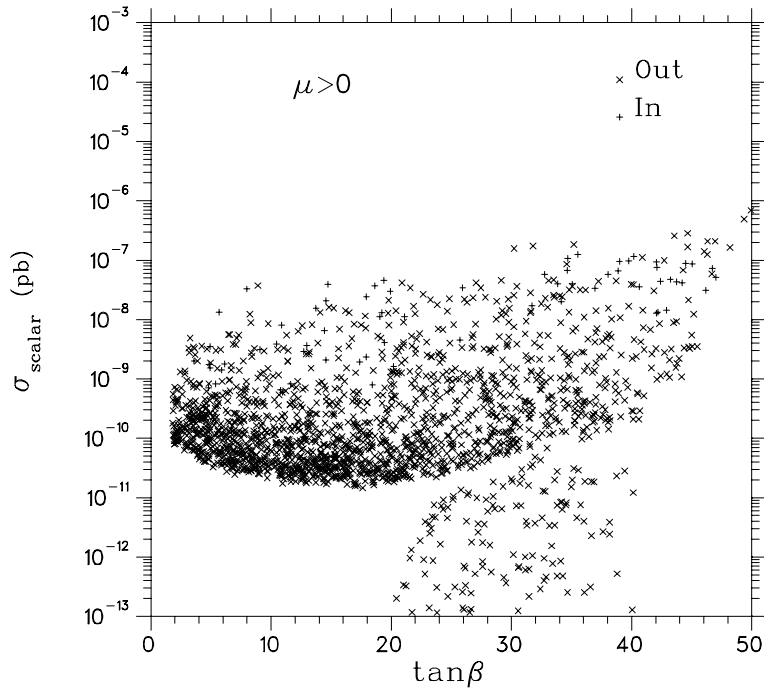


Figure 5: Scattered plot of the  $\sigma_{scalar}$  versus  $\tan\beta$  using the same random sample as in the Figure 2.